# Domain-structure relaxation in the tetragonal-to-orthorhombic phase transition of the layered perovskite $Sr_{1.8}La_{0.2}Mn_{1-y}Fe_yO_4$

Wataru Norimatsu and Yasumasa Koyama
*Department of Materials Science and Engineering, and Kagami Memorial Laboratory for Materials Science and Technology, Waseda University, Shinjuku-ku, Tokyo 169, Japan*

(Received 21 October 2006; revised manuscript received 17 December 2006; published 21 March 2007)

An *in situ* observation of the tetragonal-to-orthorhombic phase transition in Fe-substituted $Sr_{1.8}La_{0.2}MnO_4$ by transmission electron microscopy revealed that the domain structure changes, as a relaxation phenomenon, took place during the aging for the formation of the orbital ordered state. At each aging temperature, the final banded domain structure could be produced from any starting state. The characteristic features of the domain-structure relaxation found in this study are also discussed in terms of a coupling between the local Jahn-Teller and long-range dilational distortions.

DOI: 10.1103/PhysRevB.75.104416 PACS number(s): 75.47.Lx, 68.18.Jk, 68.37.Lp, 71.38.−k

## I. INTRODUCTION

The layered perovskite manganite $Sr_2MnO_4$ is an insulator, having $Mn^{4+}$ ions with an electronic configuration of $t_{2g}^3$.[1] When the $Sr^{2+}$ ions are partially replaced by $R^{3+}$ ions such as $La^{3+}$ and $Nd^{3+}$, $e_g$ electrons are doped into the system by the appearance of $Mn^{3+}$ ions. In the strongly correlated electronic manganite $Sr_{2-x}R_xMnO_4$, both the spatial distribution and the orbital occupation of $e_g$ electrons in a two-dimensional $MnO_2$ layer are of special interest.[2–9] Our previous study on $Sr_{2-x}La_xMnO_4$ showed that the doping of $e_g$ electrons leads to an orbital ordered (OO) state lacking charge ordering for $0.10 \leqslant x \leqslant 0.20$, and possessing an incommensurate charge and orbital ordered (ICOO) state for $0.20 \leqslant x \leqslant 0.50$.[10] In other words, the OO state, prior to the ICOO state, is evidently a dilute state in an $e_g$-electron system, which is characterized by the $e_g$-electron occupation of either the $(3x^2-r^2)$ or the $(3y^2-r^2)$ orbital. Because the orbital ordering accompanies a Jahn-Teller (JT) distortion, the OO state can be identified as a ferrodistortive state having orthorhombic $(O)$ symmetry.[11]

We had already conducted *in situ* observations for the disordered tetragonal (DT)-to-OO phase transition by transmission electron microscopy, and found a unique domain-structure evolution, resembling a spinodal decomposition for a compositional modulation.[10,12] The notable feature of this evolution was that, at each temperature, a sample annealing for about 1 h was needed to obtain a final domain structure. Ahn and co-workers have theoretically predicted for the presence of a relaxation process in the formation of a domain structure, produced by a coupling between the short-wavelength JT distortion and the long-wavelength distortion.[13] However, a direct observation of such a process has not yet been carried out. We have thus investigated systematically the crystallographic features of a relaxation process at each aging temperature during the DT-to-OO transition by transmission electron microscopy. Fe-substituted $Sr_{1.8}La_{0.2}Mn_{1-y}Fe_yO_4$ samples were used in this study. The adoption of the La content of $x=0.2$ is based on the experimental requirement that, in low-temperature *in situ* observations, good stability of sample temperature during an aging could be obtained around 90 K by using the liquid $N_2$ as a coolant. Because Fe-free $Sr_{1.8}La_{0.2}MnO_4$ samples exhibit the DT-to-ICOO-to-OO successive transitions, further, a main purpose of Fe substitution is the suppression for the appearance of the ICOO state.

## II. EXPERIMENTAL PROCEDURE

In the present sample preparation, we adopted a coprecipitation technique using citric acid to obtain homogeneous $Sr_{1.8}La_{0.2}Mn_{1-y}Fe_yO_4$ samples with $0 \leqslant y \leqslant 0.07$. The detailed preparation procedure, including $SrCO_3$, $La_2O_3$, $MnCO_3$, and $Fe_2O_3$ initial powders, was provided in our previous paper.[10] The crystallographic features of both the phase transitions and the relaxation processes in the prepared samples were examined by *in situ* observations with a JEM-3010-type transmission electron microscope equipped with a liquid-He-cooled holder. These observations were carried out between room temperature and 15 K. Thin specimens for *in situ* observation were made by an Ar-ion thinning method, and imaging plates were used as a recording medium in this study.

## III. RESULTS AND DISCUSSION

The phase diagram on the Fe-poor side, determined on the basis of the *in situ* observations, is shown in Fig. 1, together with dark-field images indicating the DT, ICOO, and OO states in a $y=0.01$ sample prepared in this study. As the diagram indicates, the ICOO state is stable only with very small Fe contents, and disappears just beyond $y=0.01$. However, the transition temperatures of the ICOO-to-OO and DT-to-OO transitions decrease slowly for $0 \leqslant x \leqslant 0.03$, and the OO state exists for $0 \leqslant x < 0.06$. In addition to these features, because other phenomena such as the formation of high spin complexes were not detected in this study, Fe substitution gave us samples appropriate for *in situ* observation of the DT-to-OO transition.

In the above images, fringes with a periodicity of about $9.8d_{110}$ can be seen as a microstructure in the ICOO state. In contrast, the OO state exhibits a banded structure consisting of an alternating array of two orthorhombic variants with different $b/a$ values. The characteristic feature of the Fe-

 

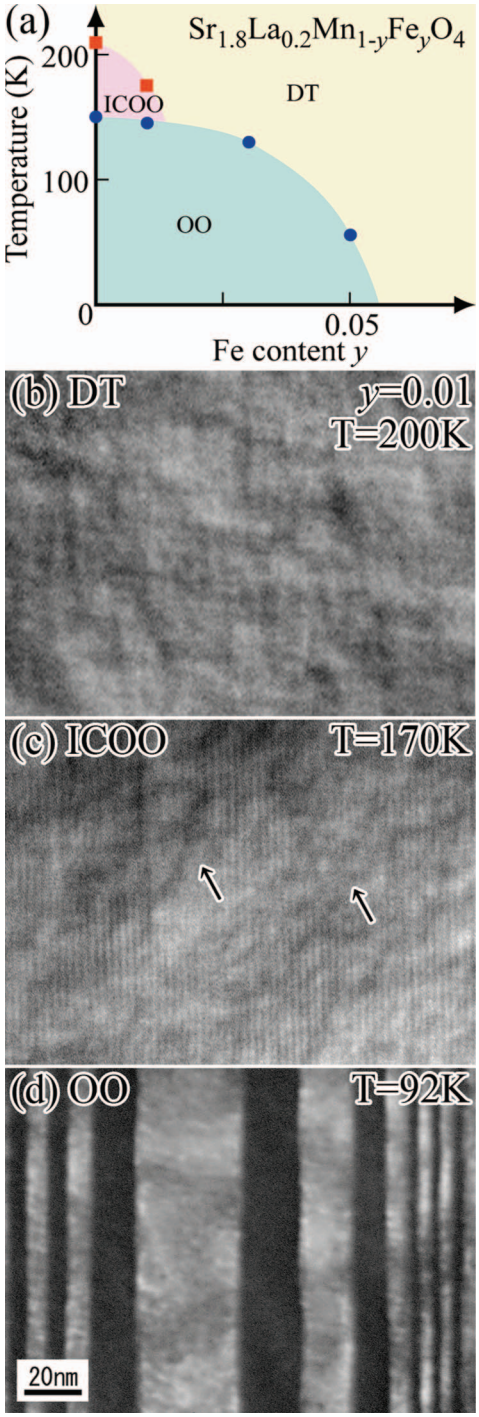


FIG. 1. (Color) Experimentally determined $Sr_{1.8}La_{0.2}Mn_{1-y}Fe_yO_4$ phase diagram for $0 \leqslant y \leqslant 0.07$, together with dark-field images of the disordered tetragonal (DT), incommensurate charge and orbital ordered (ICOO), and orbital ordered (OO) states for $y=0.01$. The images at (b) 200 K (DT), (c) 170 K (ICOO), and (d) 92 K (OO) were, respectively, taken with the 200 reflection, the 200 and surrounding satellite reflections, and the 660 reflection, due to one orthorhombic variant. The electron-beam incidence for these images was parallel to the [001] direction. In this paper, both reflections and electron incidences in electron-diffraction patterns are indexed in terms of pseudotetragonal notation.

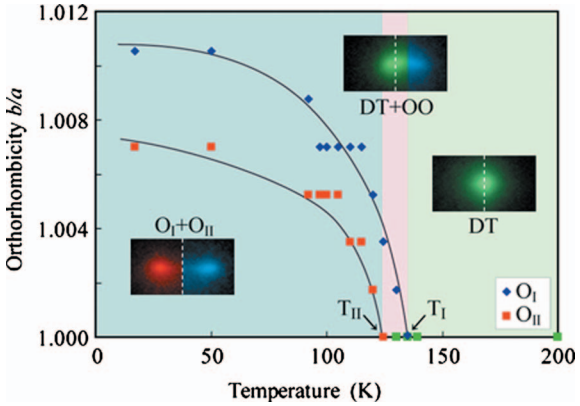


FIG. 2. (Color) Variation of $b/a$ values of two orthorhombic variants, $O_{\mathrm{I}}$ and $O_{\mathrm{II}}$, during the tetragonal-to-orthorhombic phase transition in $y=0.03$. Shown in the inset are the electron-diffraction patterns scanned at the 660 position in the [110] direction. The $b/a$ values at each temperature were determined from locations of the 660 reflections due to the $O_{\mathrm{I}}$ and $O_{\mathrm{II}}$ variants in the electron-diffraction pattern. The temperatures, where the $b/a$ values of the $O_I$ and $O_{\mathrm{II}}$ variants deviate from zero, are specified as $T_I$ and $T_{\mathrm{II}}$, respectively.

substituted sample is that the fringes in the ICOO state are obscured in several areas, indicated by the arrows. In the image of the DT state, there is a so-called tweed pattern, which indicates the presence of nanometer-sized JT clusters in the DT state. Except for the obscure fringes in the ICOO state, these microstructures appear to be identical to those in $Sr_{2-x}La_xMnO_4$, which were reported in our previous paper.[10]

The crystallographic features of the relaxation process at each temperature during the DT-to-OO phase transition were examined using a $y=0.03$ sample. The reasons for the adoption of the $y=0.03$ sample are, first, that there is no ICOO state for $y=0.03$, and second, that the transition temperature of the DT-to-OO transition is not significantly changed, even when the Fe content deviates slightly from $y=0.03$. In other words, we expected that the DT-to-OO transition would occur uniformly over a wide area of the sample. In Fig. 2, we note a variation of the $b/a$ values of the two orthorhombic variants, $O_{\mathrm{I}}$ and $O_{\mathrm{II}}$, during the DT-to-OO transition for $y=0.03$. The $b/a$ values at each temperature were obtained after the sample had been kept at that temperature for about 1 h. When the temperature of the sample in the DT state was lowered from room temperature, the $b/a$ value of the $O_{\mathrm{I}}$ variant deviated from zero only at around 135 K, $T_{\mathrm{I}}$, and a further cooling resulted in a nonzero value for the $O_{\mathrm{II}}$ variant at around 125 K, $T_{\mathrm{II}}$. The $y=0.03$ sample thus consisted of the (DT+OO) coexistence state for $T_{\mathrm{I}} \geqslant T \geqslant T_{\mathrm{II}}$ and the ($O_{\mathrm{I}}$ +$O_{\mathrm{II}}$) state for $T_{\mathrm{II}} \geqslant T$. Based on this result, we selected four aging temperatures, $T_1=140\ \mathrm{K} > T_{\mathrm{I}}$, $T_{\mathrm{I}} > T_2=130\ \mathrm{K} > T_{\mathrm{II}}$, $T_{\mathrm{II}} > T_3=92$ K, and $T_{\mathrm{II}} \geqslant T_4=15$ K, for the examination of the relaxation process in the DT-to-OO transition.

Figure 3 shows a series of dark-field images indicating the domain-structure changes during the relaxation processes at $T_1$, $T_2$, $T_3$, and $T_4$ for $y=0.03$, together with a time-temperature diagram of the thermal-treatment procedure for each process. As indicated in the (a) diagram, in the cases of

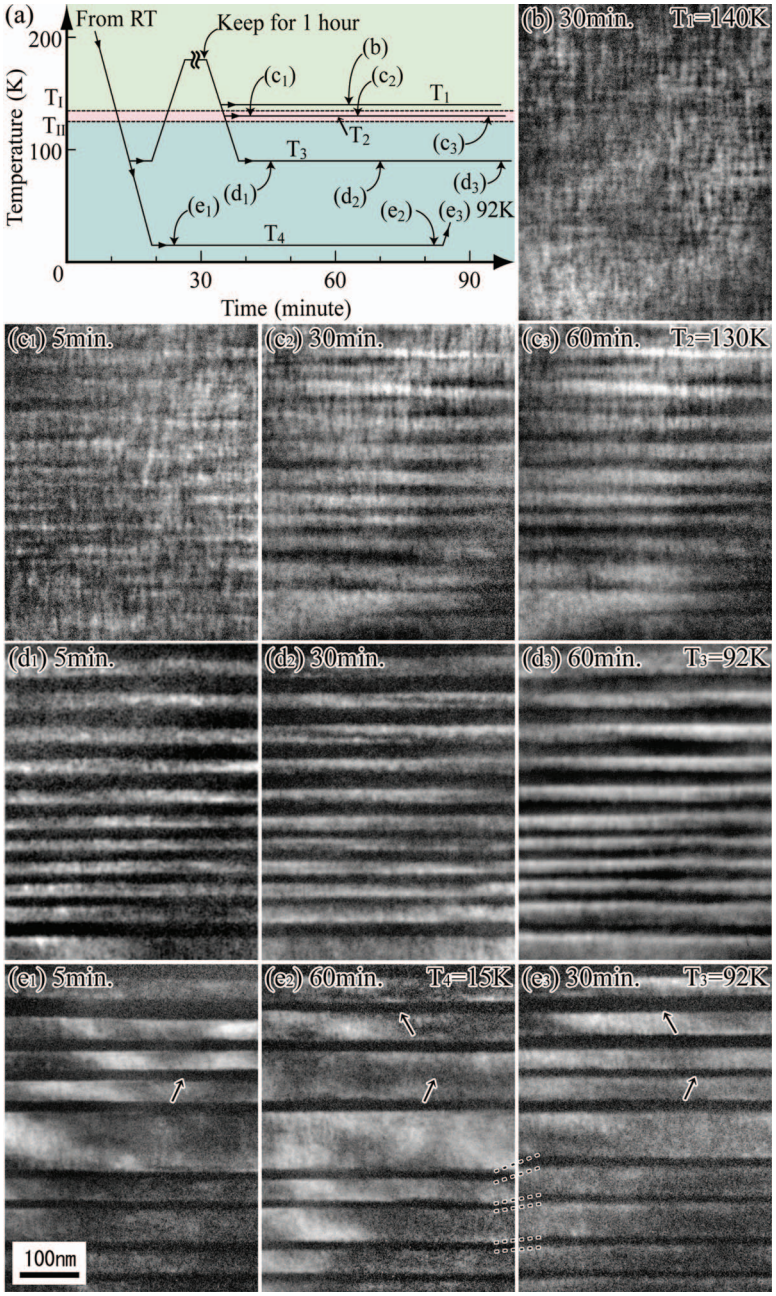


FIG. 3. (Color) A series of dark-field images indicating the domain-structure change in each relaxation process for $y=0.03$, together with a time-temperature diagram of the heat-treatment procedure. All images were taken with the 660 reflection of the DT state or the $O_{II}$ variant in the [001] electron incidence. The relaxation processes at $T_1=140$ K, $T_2=130$ K, $T_3=92$ K, and $T_4=15$ K are, respectively, shown in the (b) images, the $(c_1)$, $(c_2)$, and $(c_3)$ images, the $(d_1)$, $(d_2)$, and $(d_3)$ images, and the $(e_1)$ and $(e_2)$ images. The aging times for these images are indicated in diagram (a). In addition, the $(e_3)$ image was taken after the state shown in the $(e_2)$ image was heated and kept at $T_3$ for 30 min.

the three aging temperatures, $T_1$, $T_2$, and $T_3$, the sample was first cooled from room temperature and kept at 90 K for 15 min. This time was needed because of sample drift on cooling and sample vibration due to bubbling of the liquid $N_2$ used as a coolant. We then heated and kept the sample at 180 K for 1 h to get a starting DT state; next, we cooled it and kept it at each aging temperature, with cooling and heating rates of about 15 K/min. As for the process at $T_4$, on the other hand, the sample was directly cooled down to $T_4$, because of our experimental limitations.

We describe here the detailed features of the domain-structure change in each relaxation process. The starting DT state at 180 K had a microstructure characterized by the tweed pattern, although experimental data concerning this are not shown here. When the sample was cooled from 180 K to $T_1=140$ K $>T_I$, the tweed pattern was still observed, as seen in the (b) image for the 30-min aging. Although the pattern slightly changed during the aging, a domain structure did not form, even upon aging for more than 1 h. In other words, there was no relaxation process in the

DT state above $T_I$. The formation of a domain structure occurred during aging at $T_2=130$ K, between $T_I$ and $T_{II}$. The $(c_1)$ image taken just after cooling to $T_2$ exhibits the tweed pattern. But the subsequent aging at $T_2$ led to the appearance and development of $O_I$ bands with a (110) interface to the DT matrix, as seen in the $(c_2)$ and $(c_3)$ images. Note that the tweed pattern was still detected in the DT matrix. The sample, having aged at $T_2$ for about 1 h, thus consisted of a (DT+OO) coexistence state. In the case of the aging at $T_3$ below $T_{II}$, a banded structure characterized by an alternating array of the $O_I$ and $O_{II}$ bands had already been present in the starting state. A contrast difference between the two neighboring $O_I$ and $O_{II}$ bands became more conspicuous with aging time, as shown in images $(d_1)$, $(d_2)$, and $(d_3)$. In other words, the aging resulted in a sharpening of the boundary between the $O_I$ and $O_{II}$ bands, which is most likely related to the increase in the $b/a$ values of the $O_I$ and $O_{II}$ variants during aging. Note also that, after obtaining the $(O_I+O_{II})$ banded structure by aging at $T_3$ for 1 h, we heated and kept the sample at $T_2$ in the (DT+OO) coexistence state. As a result of aging at $T_2$, we could confirm that the $(O_I+O_{II})$ structure had converted into the $(DT+O_I)$ banded structure shown in the $(c_3)$ image.

The starting state at the aging temperature $T_4$ was the $(O_I+O_{II})$ banded structure with a sharp boundary. Both the annihilation and the thinning of the bands occurred during aging at $T_4$, as indicated by the arrows in images $(e_1)$ and $(e_2)$. To examine the domain-structure change in the $(O_I+O_{II})$ state, we heated and kept the banded domain structure at $T_3$, obtained by aging at $T_4$. An image of the sample aged at $T_3$ for 30 min is shown in image $(e_3)$. The striking feature of the domain-structure change is that, in addition to both the appearance and the widening of the bands, a movement of the bands occurred along a direction perpendicular to the boundary, as indicated by the arrows and the dashed lines. This change suggests that the number of bands in a unit length, referred to as a band density, has an aging-temperature dependence in the $(O_I+O_{II})$ banded domain structure.

When the sample, originally in the DT state, was cooled and kept at each aging temperature, three relaxation processes were observed as the domain-structure change to the final $(DT+O_I)$ or $(O_I+O_{II})$ banded structure. The change, produced by aging in the (DT+OO) coexistence state, was the formation of the $(DT+O_I)$ banded domain structure from the tweed-pattern state. In contrast, there were two relaxation processes associated with the formation of the $(O_I+O_{II})$ banded structure. The first was the sharpening of the boundary between the $O_I$ and $O_{II}$ bands at higher temperatures and the second was the annihilation of the bands at lower temperatures. The striking features of these relaxation processes are that the $(DT+O_I)$ domain structure is produced both from the tweed-pattern state and from the $(O_I+O_{II})$ banded structure, and that the band density in the $(O_I+O_{II})$ structure depends upon the aging temperature in the OO state. The latter feature, in particular, is unusual because the raising of the aging temperature in the OO state results in both the appearance and the movement of the bands. Evidently, the formation of the OO state in the layered manganite accompanies these curious relaxation processes. Thus we here discuss the origin of the appearance of the domain-structure relaxation in terms of a coupling between the local JT and long-range distortions.

We first establish the order parameter in the DT-to-OO transition. Because the transition is characterized by orbital ordering only, the occupation of the $(3x^2-r^2)$ or $(3y^2-r^2)$ orbital by $e_g$ electrons can be identified as an electronic order parameter in the transition. The corresponding local JT distortion constitutes a structural order parameter on the basis of a strong electron-lattice coupling. The important point to note here is that the local JT distortion for the electronic order parameter is associated with a reducible representation in the $D_{4h}$ group of the DT state. This reducible representation, corresponding to the $E_g$ irreducible representation of the $O_h$ group, should reduce to the $A_{1g}$ and $B_{1g}$ irreducible representations in the Koster notation.[14] This implies that the local JT distortion can be coupled to both the long-range $A_{1g}$ dilational distortion $(e_{xx}+e_{yy})$ and the $B_{1g}$ $O$ distortion $(e_{xx}-e_{yy})$ in the $MnO_2$ layer. Notably, due to the dilational distortion, an expanded area produced by the presence of an OO region results in a contracted area around it. In the contracted area, the development of JT clusters, accompanying a lattice expansion, is strongly suppressed. That is, the (DT+OO) coexistence state can be explained as being due to the presence of the dilational distortion. With such distortion present, a coupling between the JT and long-range distortions is most likely responsible for the unusual structural characteristics found in this study.

Here, the following point should be remarked. A similar domain-structure evolution was found in the spinodal decomposition of alloys.[12] In the decomposition, a compositional modulation occurs when a metastable alloy of a single phase is aged in a two-phase region of the phase diagram. The domain-structure evolution in the decomposition is then associated with a compositional modulation. Given this background, our interest is focused on what mechanism produces the similarity between the formation of the OO state and the compositional modulation. One possible factor is likely to be a dilational distortion. In the decomposition process, a change in the concentration leads to a change in the lattice parameter manifesting as a dilational distortion. As Khachaturyan pointed out theoretically, the domain-structure evolution in the decomposition could be explained as being due only to a strain-field effect related to a dilational distortion.[15] This attribution suggests that, although the OO-state formation and the spinodal decomposition occur, respectively, through the orbital occupation of $e_g$ electrons and the site occupation of atoms, the dilational distortions produced by these occupations play an essential role in such domain-structure changes.

With the similarity to the spinodal decomposition in mind, we now discuss the domain-structure evolution in the layered manganite. To interpret the evolution, we first pay attention to the fact that $O_I$ bands with a $(3x^2-r^2)$ orbital ordering were formed in the DT state, occurring as stripes of about 10 nm in width, arranged quasiperiodically with a spacing of about 50 nm along the [110] direction. This finding presumably implies that some $e_g$-electron concentration may go to

the narrow $O_{\mathrm{I}}$ bands, while the broader 50-nm strips of the DT state would be less concentrated. Consequently, the DT state is changed into $O_{\mathrm{II}}$ bands with the $(3y^2-r^2)$ ordering at lower temperatures, which acquire lower orthorhombicity. At the lowest temperatures, the $e_g$ electrons are redistributed, and the $O_{\mathrm{I}}$ and $O_{\mathrm{II}}$ bands tend to form a unique orbitally ordered state.

## IV. CONCLUSION

In summary, a relaxation phenomenon, observed as a domain-structure change, was found to occur during the DT-to-OO phase transition of a strongly correlated electronic manganite considered as an $e_g$-electron system. The appearance of the relaxation processes is most likely due to a coupling between the local JT and long-range dilational distortions. The notable feature of the processes is that, with each aging temperature, any starting state led to the same final domain structure. In addition, the appearance and movement of the bands occurred when the aging temperature was raised in the OO state. It is thus suggested that the characteristics of the banded domain structures in the OO state, such as their band densities, are temperature dependent.

[1] J. Bouloux, J. Soubeyroux, G. Flem, and P. Hagenguller, J. Solid State Chem. **38**, 34 (1981).
[2] Y. Moritomo, Y. Tomioka, A. Asamitsu, Y. Tokura, and Y. Matsui, Phys. Rev. B **51**, 3297 (1995).
[3] Y. Moritomo, A. Nakamura, S. Mori, N. Yamamoto, K. Ohoyama, and M. Ohashi, Phys. Rev. B **56**, 14879 (1997).
[4] W. Bao, C. H. Chen, S. A. Carter, and S.-W. Cheong, Solid State Commun. **98**, 55 (1996).
[5] S. Larochelle, A. Mehta, N. Kaneko, P. K. Mang, A. F. Panchula, L. Zhou, J. Arthur, and M. Greven, Phys. Rev. Lett. **87**, 095502 (2001).
[6] S. Larochelle, A. Mehta, L. Lu, P. K. Mang, O. P. Vajk, N. Kaneko, J. W. Lynn, L. Zhou, and M. Greven, Phys. Rev. B **71**, 024435 (2005).
[7] T. Kimura, K. Hatsuda, Y. Ueno, R. Kajimoto, H. Mochizuki, H. Yoshizawa, T. Nagai, Y. Matsui, A. Yamazaki, and Y. Tokura, Phys. Rev. B **65**, 020407(R) (2001).
[8] T. Nagai, T. Kimura, A. Yamazaki, T. Asaka, K. Kimoto, Y. Tokura, and Y. Matsui, Phys. Rev. B **65**, 060405(R) (2002).
[9] M. Daghofer, A. Oles, D. Neuber, and W. von der Linden, Phys. Rev. B **73**, 104451 (2006).
[10] W. Norimatsu and Y. Koyama, Phys. Rev. B **74**, 085113 (2006).
[11] Y. Yamada and T. Takakura, J. Phys. Soc. Jpn. **71**, 2480 (2002).
[12] Y. Koyama, Acta Metall. Mater. **38**, 857 (1990).
[13] K. H. Ahn, T. Lookman, and A. R. Bishop, Nature (London) **428**, 401 (2004).
[14] G. F. Koster, *Solid State Physics*, edited by F. Seitz and D. Turnbull (Academic Press Inc., New York, 1957), Vol. V.
[15] A. G. Khachaturyan, *Theory of Structural Transformations in Solids* (Wiley-Interscience, New York, 1983), Vol. 10.